

KINEMATICS AND WORKSPACE ANALYSIS OF A PARALLEL ARCHITECTURE ROBOT: THE HEXA

Sylvio Celso Tartari Filho

University of São Paulo
Dep. of Mechatronics Engineering
Av. Prof. Mello Moraes, 2231
São Paulo – SP, Brazil
sylvio.tartari@poli.usp.br
sylvioctf@ibest.com.br

Eduardo Lobo Lustosa Cabral

University of São Paulo
Dep. of Mechatronics Engineering
Av. Prof. Mello Moraes, 2231
São Paulo – SP, Brazil
elcabral@usp.br

Abstract. Many applications in the field of production automation, such as assembly and material handling, require machines capable of very high speeds and accelerations. Since 1965 with Stewart's work the parallel robots proved to be a strong supplement to the serial robots. The parallel robots are able to work on some tasks with a much better performance. However, there are still several unanswered questions and few papers published studying robots with parallel architectures. It is in this environment that this work fits in: focusing on the study of the inverse kinematics. First a kinematics model of a Hexa parallel machine is obtained using a generic geometrical formulation then the model is used for a workspace analysis. The reachable workspace of a Hexa machine is calculated given some restrictions such as the collision avoidance of the links, angular limitations of the joints and angular pose requirements that the moving platform must fulfill. Other types of workspaces, like the constant orientation and the total orientation, are also discussed. To show the results a virtual environment to simulate the Hexa architecture was built using the Matlab 6.5 platform. The simulator is capable of handling usual operations of a real Hexa machine, like linear and circular trajectories in any direction, the use of a global coordinate system or a local one placed in the mobile platform, and changes of orientation during movement.

Keywords: parallel architecture, robot, kinematics, workspace, Hexa.

1. Introduction

The first known parallel robot was designed as a solution to the competition *Le Prix Vaillant*, which took place in France, in the early 1900's. The main problem was to determine under which circumstances a rigid body could demonstrate the capacity of executing continuous movements when some of its points were obligated to remain over fixed spheres, which is the basic concept of the parallel robots. Only in 1947, Gough established the basic principles of a closed loop mechanism, and in 1955 built a prototype, with the purpose of tire testing (Gough 1957, 1962). However, the parallel robots became famous only after Stewart's suggestion to use one as a flight simulator in the 60's (Stewart, 1965). Due to this usage, Gough's platform is wrongly known as Stewart's platform. After that, the interest on those robots raised, being studied also for applications in industry (milling, pick-and-place...), medical (surgeries) and others.

The focus of this work is the six degrees of freedom (d.o.f) Hexa robot, proposed by Uchiyama (1994), which is actually an extended concept of the 3 d.o.f. Delta robot, proposed by Pierrot (1991). In the Hexa robot the actuated revolute joints are responsible for the movement of six rods (actuated rods), which are linked to other six rods (passive rods) by spherical joints. Lastly, these passive rods are also linked to the moving platform by spherical joints. By controlling the actuated rods movement it is possible to control the moving platform that carries the end-effector.

Hexa's design is perfect for pick-and-place operations, having a light structure and being capable of reaching high speeds and accelerations. In this work a study and analysis of Hexa robot's inverse kinematics and workspace are presented for the purpose of building a simulator and serving as a basis for further researches in parallel robotics, especially in synthesis and optimization.

Figure 1 presents three machines: Gough's platform and the Delta and Hexa architectures robots.



Figure 1. From left to right: Gough's Platform; ABB FlexPicker™ (Delta Architecture); Hexa from IWF

2. Inverse Kinematics

The inverse kinematics equations relate the position of the end-effector with the actuators coordinates. The structure presented in Fig. 2 is a schematic of the Hexa architecture. The set of points shown as $Pi_j = \{Pi_1, Pi_2, \dots, Pi_6\}$ represents the centers of the spherical joints that link the passive rods to the moving platform; the set $Pa_j = \{Pa_1, Pa_2, \dots, Pa_6\}$ represents the centers of the universal joints that links the actuated rods to the passive ones; finally the set $Ps_j = \{Ps_1, Ps_2, \dots, Ps_6\}$ represents the centers of the revolute actuated joints. The point Pc is the point in which all movements are based from (for instance, a tool tip). The coordinate system $o-xyz$ has its origin in Pc and is fixed to the moving platform. $O-XYZ$ is global, being fixed in the base. The set of actuated and passive links are, respectively, $l_j = \{l_1, l_2, \dots, l_6\}$ and $h_j = \{h_1, h_2, \dots, h_6\}$.

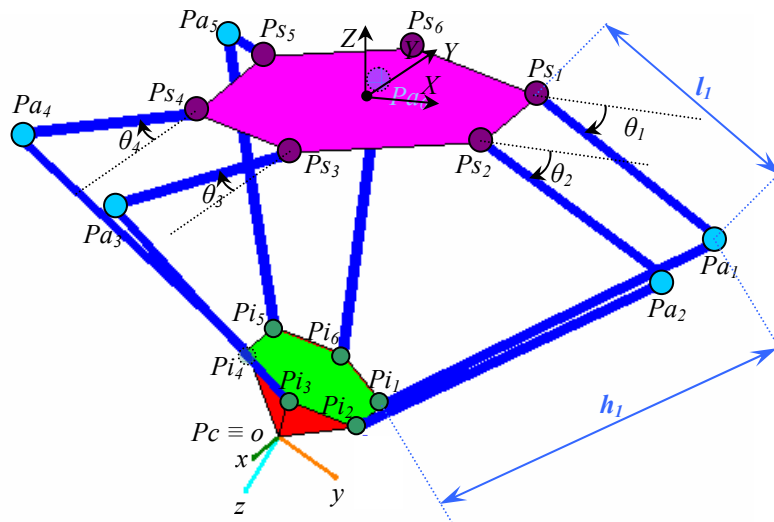


Figure 2. Hexa's moving platform and fixed base

To obtain the inverse kinematic equations it is possible to use the Denavit-Hartenberg method, although the geometrical method is much simpler to use (Tsai, 1999), being the one described next.

A relationship can be established between the points Pa_j and Ps_j , in the $O-XYZ$ coordinate system. Using the actuator's position $\theta_j = \{\theta_1, \theta_2, \dots, \theta_6\}$, it follows:

$$\begin{bmatrix} x_{Pa_1} \\ y_{Pa_1} \\ z_{Pa_1} \end{bmatrix} = \begin{bmatrix} x_{Ps_1} \\ y_{Ps_1} \\ z_{Ps_1} \end{bmatrix} + \begin{bmatrix} l_1 \cdot \cos \theta_1 \\ 0 \\ -l_1 \cdot \sin \theta_1 \end{bmatrix} \quad (1)$$

$$\begin{bmatrix} x_{Pa_2} \\ y_{Pa_2} \\ z_{Pa_2} \end{bmatrix} = \begin{bmatrix} x_{Ps_2} \\ y_{Ps_2} \\ z_{Ps_2} \end{bmatrix} + \begin{bmatrix} l_2 \cdot \cos \theta_2 \\ 0 \\ -l_2 \cdot \sin \theta_2 \end{bmatrix} \quad (2)$$

$$\begin{bmatrix} x_{Pa_3} \\ y_{Pa_3} \\ z_{Pa_3} \end{bmatrix} = \begin{bmatrix} x_{Ps_3} \\ y_{Ps_3} \\ z_{Ps_3} \end{bmatrix} + \begin{bmatrix} -l_3 \cdot \cos 60^\circ \cdot \cos \theta_3 \\ -l_3 \cdot \sin 60^\circ \cdot \cos \theta_3 \\ -l_3 \cdot \sin \theta_3 \end{bmatrix} \quad (3)$$

$$\begin{bmatrix} x_{Pa_4} \\ y_{Pa_4} \\ z_{Pa_4} \end{bmatrix} = \begin{bmatrix} x_{Ps_4} \\ y_{Ps_4} \\ z_{Ps_4} \end{bmatrix} + \begin{bmatrix} -l_4 \cdot \cos 60^\circ \cdot \cos \theta_4 \\ -l_4 \cdot \sin 60^\circ \cdot \cos \theta_4 \\ -l_4 \cdot \sin \theta_4 \end{bmatrix} \quad (4)$$

$$\begin{bmatrix} x_{Pa_5} \\ y_{Pa_5} \\ z_{Pa_5} \end{bmatrix} = \begin{bmatrix} x_{Ps_5} \\ y_{Ps_5} \\ z_{Ps_5} \end{bmatrix} + \begin{bmatrix} -l_5 \cdot \cos 60^\circ \cdot \cos \theta_5 \\ l_5 \cdot \sin 60^\circ \cdot \cos \theta_5 \\ -l_5 \cdot \sin \theta_5 \end{bmatrix} \quad (5)$$

$$\begin{bmatrix} x_{Pa_6} \\ y_{Pa_6} \\ z_{Pa_6} \end{bmatrix} = \begin{bmatrix} x_{Ps_6} \\ y_{Ps_6} \\ z_{Ps_6} \end{bmatrix} + \begin{bmatrix} -l_6 \cdot \cos 60^\circ \cdot \cos \theta_6 \\ l_6 \cdot \sin 60^\circ \cdot \cos \theta_6 \\ -l_6 \cdot \sin \theta_6 \end{bmatrix} \quad (6)$$

Using the passive rods edge coordinates, it is possible to establish the following relation:

$$h_j^2 = (x_{Pa_j} - x_{Pi_j})^2 + (y_{Pa_j} - y_{Pi_j})^2 + (z_{Pa_j} - z_{Pi_j})^2 \quad (7)$$

Using now Eq. (1) until (6) into Eq. (7), it is possible to arrive at the following relations:

$$h_1^2 = (x_{Ps_1} - x_{Pi_1} + l_1 \cos \theta_1)^2 + (y_{Ps_1} - y_{Pi_1})^2 + (z_{Ps_1} - z_{Pi_1} - l_1 \sin \theta_1)^2 \quad (8)$$

$$h_2^2 = (x_{Ps_2} - x_{Pi_2} + l_2 \cos \theta_2)^2 + (y_{Ps_2} - y_{Pi_2})^2 + (z_{Ps_2} - z_{Pi_2} - l_2 \sin \theta_2)^2 \quad (9)$$

$$h_3^2 = (x_{Ps_3} - x_{Pi_3} - l_3 \cos 60^\circ \cos \theta_3)^2 + (y_{Ps_3} - y_{Pi_3} - l_3 \sin 60^\circ \cos \theta_3)^2 + (z_{Ps_3} - z_{Pi_3} - l_3 \sin \theta_3)^2 \quad (10)$$

$$h_4^2 = (x_{Ps_4} - x_{Pi_4} - l_4 \cos 60^\circ \cos \theta_4)^2 + (y_{Ps_4} - y_{Pi_4} - l_4 \sin 60^\circ \cos \theta_4)^2 + (z_{Ps_4} - z_{Pi_4} - l_4 \sin \theta_4)^2 \quad (11)$$

$$h_5^2 = (x_{Ps_5} - x_{Pi_5} - l_5 \cos 60^\circ \cos \theta_5)^2 + (y_{Ps_5} - y_{Pi_5} + l_5 \sin 60^\circ \cos \theta_5)^2 + (z_{Ps_5} - z_{Pi_5} - l_5 \sin \theta_5)^2 \quad (12)$$

$$h_6^2 = (x_{Ps_6} - x_{Pi_6} - l_6 \cos 60^\circ \cos \theta_6)^2 + (y_{Ps_6} - y_{Pi_6} + l_6 \sin 60^\circ \cos \theta_6)^2 + (z_{Ps_6} - z_{Pi_6} - l_6 \sin \theta_6)^2 \quad (13)$$

Equations (8) until (13) can be written in the format $a = b \cdot \cos \theta + c \cdot \sin \theta$, so that:

$$\theta = \arctan \left[\frac{\left[a \cdot c^2 - b \cdot \sqrt{-c^2 \cdot (a^2 - b^2 - c^2)} \right] / \left[c \cdot (b^2 + c^2) \right]}{\left[a \cdot b + \sqrt{-c^2 \cdot (a^2 - b^2 - c^2)} \right] / (b^2 + c^2)} \right] \quad (14)$$

For each equation from Eq. (8) until Eq. (13) there is a different set of parameters a , b and c . Equations (15), (16) and (17) describe these parameters, respectively, for Eq. (8) and (9), (10) and (11), and (12) and (13).

$$\begin{aligned} a &= \frac{h_j^2 - l_j^2 - (x_{Ps_j} - x_{Pi_j})^2 - (y_{Ps_j} - y_{Pi_j})^2 - (z_{Ps_j} - z_{Pi_j})^2}{2 \cdot l_j} \\ b &= (x_{Ps_j} - x_{Pi_j}) \\ c &= -(z_{Ps_j} - z_{Pi_j}) \end{aligned} \quad (15)$$

$$\begin{aligned}
 a &= \frac{h_j^2 - l_j^2 - (x_{Ps_j} - x_{Pi_j})^2 - (y_{Ps_j} - y_{Pi_j})^2 - (z_{Ps_j} - z_{Pi_j})^2}{l_j} \\
 b &= -\left[\sqrt{3} \cdot (y_{Ps_j} - y_{Pi_j}) + (x_{Ps_j} - x_{Pi_j}) \right] \\
 c &= -2 \cdot (z_{Ps_j} - z_{Pi_j})
 \end{aligned} \tag{16}$$

$$\begin{aligned}
 a &= \frac{h_j^2 - l_j^2 - (x_{Ps_j} - x_{Pi_j})^2 - (y_{Ps_j} - y_{Pi_j})^2 - (z_{Ps_j} - z_{Pi_j})^2}{l_j} \\
 b &= \sqrt{3} \cdot (y_{Ps_j} - y_{Pi_j}) - (x_{Ps_j} - x_{Pi_j}) \\
 c &= -2 \cdot (z_{Ps_j} - z_{Pi_j})
 \end{aligned} \tag{17}$$

The set of points P_{S_j} are fixed, being part of the fixed base. Given the position (defined by P_c) and the orientation of the moving platform, with respect to the coordinate system $O-XYZ$, it is possible to calculate the points P_{i_j} . Using both sets (P_{S_j} and P_{i_j} for $j = 1, 2, \dots, 6$) and Eq. (14) until (17), the actuators' position are calculated. Then, by using Eq. (1) until (6), the positions of the intermediate joints are calculated (the set P_{a_j}). In brief, from the moving platform coordinates (P_c and P_{i_j}) it is possible to obtain the actuators' position.

3. Workspace

Workspace is the reachable portion of space by the end-effector's interest point, respecting some requirements. In other words, there is not a single type of workspace; it depends on what is required. In this work two kinds of workspaces are considered: the *constant orientation* and the *total orientation*, as described by Merlet (2000). The first one is the reachable space by the moving platform for a certain fixed pre-defined orientation, also called the translational workspace. The second one is the reachable space by the moving platform in which it is possible to achieve all the orientations among a given set of them. In this work it is considered any orientation in any direction by a certain desired angle (excluding rotations around the z axis). There are several other types of workspace that can even be custom defined, but those are not part of this paper's scope. Just as an example is the Force Transmission Factor Workspace, studied by several researchers. Funabashi (1994) defined this workspace as the reachable space in which this factor is above a given value from anywhere from 0 to 1. The transmission factor is correspondent to the cosine of the transmitted force by the links to the moving platform and the velocity vector of the platform, being a measure of how much of the transmitted force to the moving platform is in the same direction of its movement. As another example, there is the Dextrous Workspace, defined as the set of locations of the interest point in which all moving platform orientations are possible. Actually, this is a particular case of the total orientation workspace.

To search for the workspace there are quite a few algorithms. The simplest method that can be used is to determine a sufficiently large set of locations, divide it in a three-dimensional net and then to each point verify if it is a feasible point. Obviously, this is an algorithm that requires too much computational time and therefore it is not so much efficient. For the workspace determination we used a similar method to the one applied by Conti (Conti et al. 1997). This algorithm is based on spherical coordinates. A central point C is defined and then by changing φ , λ and ρ - respectively the spherical coordinates angles and radius - the workspace boundary is found. See Fig. 3 for a graphical explanation. The main steps are:

1. Define the desired constraints and create a "Test Pose" function. In this paper the constraints are defined as the collision avoidance between links and between links and the moving platform, and also the mechanical limits of the joints, both passive and actuated. The "Test Pose" function has the current moving platform pose as an input and returns *true* if all constraints are respected or *false* if at least one constraint is not respected or if the point is not reachable with the given rods lengths. Lastly, it is important to explain that pose is understood as the moving platform position and orientation;
2. Define the acceptable error, ϵ . The algorithm searches for the workspace boundary by altering the length of ρ , and to allow the numerical routine to have a stop condition, a tolerance must be defined;
3. Define the Initial Radius R , which is the initial value for ρ . At the beginning of each algorithm's iteration, R is divided by 2 and this value is added to or subtracted from ρ , meaning that R also defines the search limits and must be large enough to allow a complete workspace search but yet small enough to allow convergence in little time. In this work R was defined as $2^*(h+l)$.
4. Determine the central point C . To determine it, first the platform is centered with respect to the coordinates X and Y , then, by varying the coordinate Z and by using the "Test Pose" function, the upper and lower limits are determined. C can be essentially any point; in this work it is considered to be in the middle of both limits. If no points are found, meaning that the platform cannot reach $(X, Y) = [0, 0]$, increment X or Y and repeat the process (this case was not found in the experiments, but it is considered in the algorithm).
5. Determine the steps for φ and λ and start the search algorithm. Use $0^\circ \leq \varphi \leq 180^\circ$ and $0^\circ \leq \lambda \leq 360^\circ$. For each pair of φ and λ , the algorithm starts with $\rho = R$ and applies the "Test Pose". If the function returns *true*, ρ is

incremented by $R/2$, otherwise ρ is decremented by $R/2$. The algorithm continues reducing the increment to $R/4, R/8 \dots$ until it is smaller than or equal to ϵ and the “Test Pose” function returns *true*. The process continues until all boundary points are found – $L_{(\phi, \lambda, \rho)}$. If the total orientation workspace is being searched, the Hexa’s symmetry along the XZ plane can be used, so λ can vary from 0° to 180° .

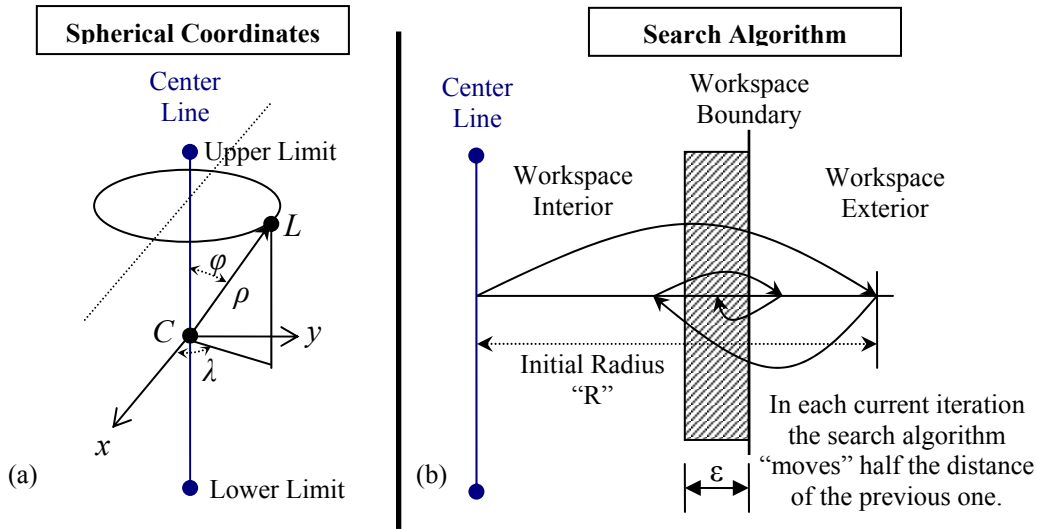


Figure 3. Workspace search algorithm: a) Spherical Coordinates and b) Algorithm

As mentioned, the following constraints are used:

a) *Angular joints limits* – The actuators position are calculated from Eq. (14) and then their limits are verified for violations. The spherical joint angles are calculated as $\{l_i\} \cdot \{h_i\} = \|\{l_i\}\| \cdot \|\{h_i\}\| \cdot \cos(\phi_i)$, thus:

$$\phi_i = \arccos\left(\frac{\{l_i\} \cdot \{h_i\}}{\|\{l_i\}\| \cdot \|\{h_i\}\|}\right), \text{ for } i = 1, 2, \dots, 6. \quad (18)$$

Where ϕ_i is the angle between linked passive and actuated rods. For the spherical joints in the moving platform the limits are shown in Fig. 4. The dashed arrow pointing out of the platform represents a normal vector that serves as a virtual reference to calculate the maximum allowed angle of the spherical joints. Also, by defining this limit, the collision between moving platform and limbs are avoided. Ψ defines the boundary (cone format) in which the passive links can be positioned with respect to the moving platform.

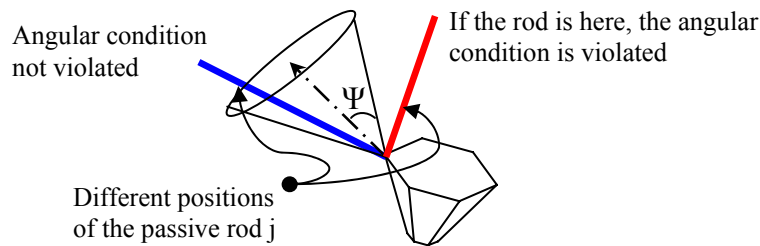


Figure 4. Angular limits of the spherical joints

b) *Avoiding elements collision* – After applying the angular limits and considering Hexa’s architecture itself, almost all types of collision are eliminated. The important one that is still missing is the collision between passive rods. For the numerical algorithm, rods are nothing more than line segments. Then, what must be done is to calculate the minimum distance between them and compare it to a minimum distance value identical to the diameter of a limb (if they have cylindrical format) or other safe distance considered. To do so, first it is verified if the two limbs are parallel. If so, they form a linearly dependent system and the distance between them is calculated like the distance between a point and a line. If they are not, then the distance is calculated normally like two lines. However, if the minimum distance found between two rods links two points of the rods that do not belong to them (remember that the concept of line is infinite), then the minimum distance calculation involves one of the rods extremities (four points): Pa_j or Pi_j , and j depends on

the rods considered. Then the distance between the rods will be the distance between one of the edges of a rod until the other rod. Remember that both points must be within Pa_j and Pi_j . Fig. 5a illustrates those considerations. After all space is searched, then the next two steps are to plot the graphics and to calculate the volume of the workspace. The algorithm will provide several points that define the workspace boundary. Due the constant steps used, the boundary shell is made of several cells defined by the surrounding four boundary points. To calculate the volume, each cell is split into two triangular ones and the point C can be perceived as the top of several pyramids. Their bases are formed by each triangular cell defined by three workspace boundary points. Summing the volume of all pyramids, the total is found. The formula is presented also in Fig. 5.

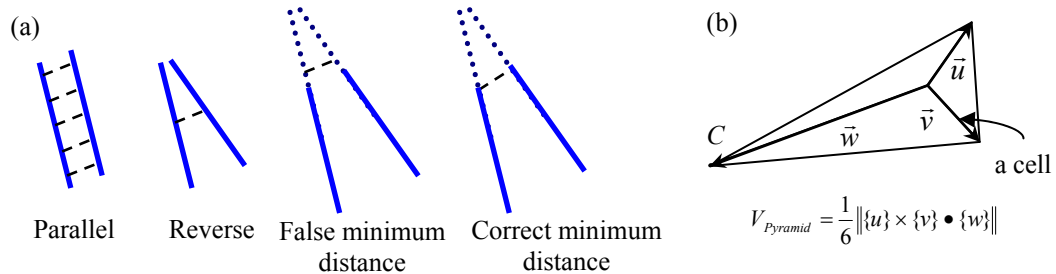


Figure 5: (a) Relative position between two limbs; (b) Pyramid Calculation

4. Development Tools

This section describes the development tools made using Matlab platform: a workspace boundary finder and a simulator for the Hexa robot, both used in this work. These tools are useful for understanding how the Hexa robot works and for the synthesis and optimization of the robot architecture. Note that these tools were developed in this work.

4.1. Geometry and Workspace Definition Tool

Figure 6 shows the main window of the Hexa Tool developed in this work. From this window it is possible to access the simulation tool and also to run the workspace finder algorithm. The first step is to define the Hexa machine geometry along with all key points. An image of the desired machine is shown as well. The desired constraints (the minimum acceptable distance between limbs and angular limitation of the joints) also serve as inputs for the workspace finder algorithm.

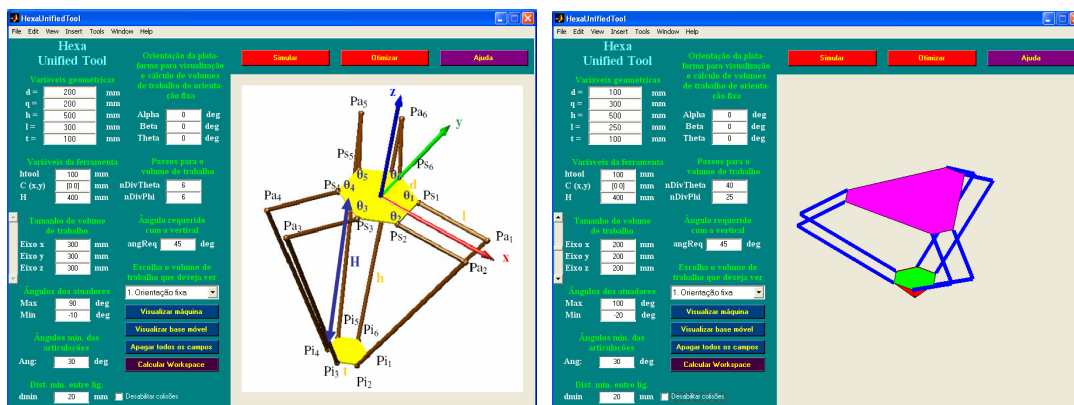


Figure 6: Main window of the Hexa Tool for Matlab

Also in the same window, the desired parameters for the workspace calculations are set. For the fixed orientation workspace there are three angles to define the platform orientation. For the total orientation, there is just the minimum angle with the Z axis, indicating that all orientations (except the ones around Z) from zero degrees to the desired angle must be deemed possible.

4.2. Simulator Tool

The developed simulator is useful to identify Hexa's workspace limitations in terms of certain common tasks that the machine has to perform while in operation. Some of the simulator features shown in Fig. 7. As shown in this figure,

the tool is capable of simulating several types of movements of the Hexa machine, such as linear and circular interpolations, in any chosen plane, and platform orientation changes in any direction using any point as center and while moving. It is also possible to use linear interpolations from the coordinate system $o-xyz$, instead of the $O-XYZ$. As outputs, the tool calculates in real-time the actuators position and the roll-pitch-yaw angles.

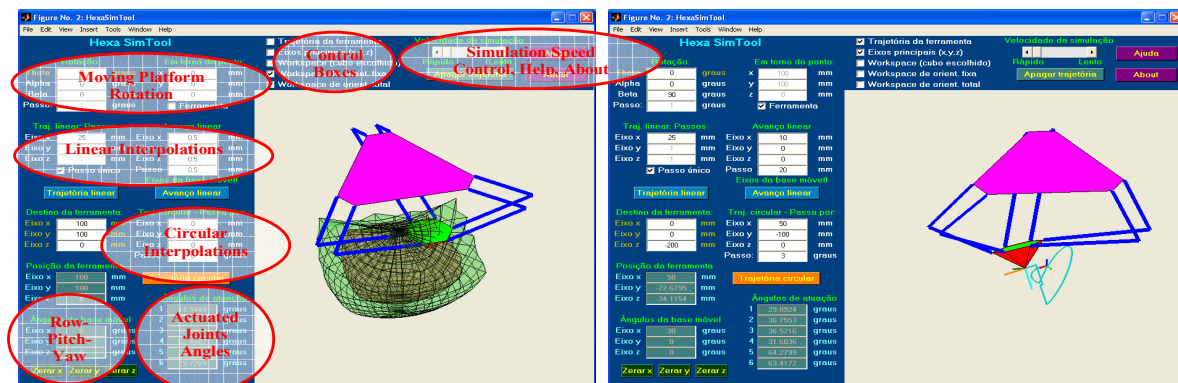


Figure 7. Developed Hexa's Simulator and some highlighted features

5. Results

For the next results, the fixed orientation angles of $[0^\circ, 0^\circ, 0^\circ]$ and the required angle for the total orientation equal to 45° are used. It was also imposed angular restrictions of $[100^\circ, -20^\circ]$ for the actuated joints (maximum and minimum angles, 30° of minimum angle for the others and a minimum distance between limbs of 20 mm. Hexa robot's dimensions are: 100 mm for the distance between each one of the three pairs of the actuated joint centers; 100 mm for the side of the moving platform (hexagonal shape); 100 mm for the tool height; 250 mm of actuated rods length; 500 mm of passive rods length; and 300 mm for the distance from the center of the fixed base to one of the actuated joints center lines.

The workspaces found for the Hexa robot are shown in Fig. 8. For a better understanding of the fixed orientation angles influence, Fig. 9 presents the workspace for the angle set $[90^\circ, 90^\circ, 45^\circ]$, i.e., 45° of rotation around Y axis. For both figures steps of 9° for λ , i.e., 40 divisions (or directions) and of 7.2° for φ (25 divisions) are used. About 30 – 40 divisions for λ and 20 – 25 divisions for φ provide very nice results. Table 1 shows the volumes of some workspace runs.

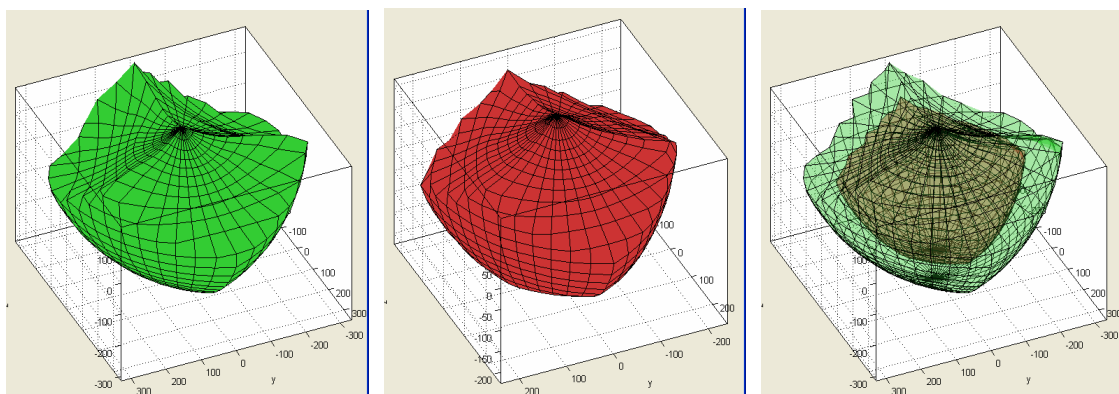


Figure 8. Hexa robot's workspaces. From left to right: fixed orientation workspace, total orientation workspace and both of them in one single picture for comparison

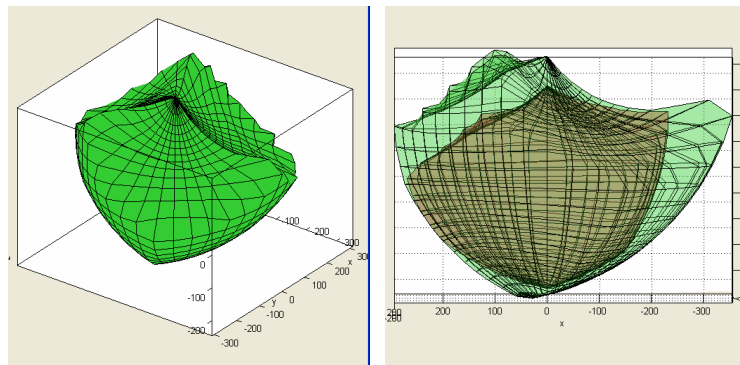


Figure 9. From left to right: Hexa robot's fixed orientation workspace and both fixed and total orientation in one single picture for comparison.

Table 1. Total workspace volumes found

Cases			Fixed Orient. (mm ³)	Total Orient. (mm ³)
N. div. λ	N. div. φ	$[\alpha, \beta, \theta]$		
40	25	$[0^\circ, 0^\circ, 0^\circ]$	8.18×10^7	3.70×10^7
30	20	$[0^\circ, 0^\circ, 0^\circ]$	8.12×10^7	3.69×10^7
6	6	$[0^\circ, 0^\circ, 0^\circ]$	6.47×10^7	3.10×10^7
40	25	$[90^\circ, 90^\circ, 45^\circ]$	6.48×10^7	3.70×10^7
30	20	$[90^\circ, 90^\circ, 45^\circ]$	6.42×10^7	3.69×10^7
6	6	$[90^\circ, 90^\circ, 45^\circ]$	5.02×10^7	3.10×10^7

6. Conclusions

The presented inverse kinematic model proves to be a simple way to solve this particular issue in parallel robotics and can be used in other types of architectures. The model is fast and is applied in real time simulations through the simulation tool. The workspace algorithm suggested in this work is also suitable for implementation and can be combined with the simulation algorithms, providing an even more advanced tool.

The developed tools are the first steps of a deeper study in parallel architecture robots. Also by proving that the tools developed so far are correct, we are moving toward our ultimate goal that is the synthesis and optimization of a Hexa machine, possibly followed by a prototype construction.

Our next steps are to obtain the dynamics model and make a Jacobian analysis for singularity detection and performance measure. Combining the kinematics, the dynamics and the Jacobian analysis we will start the synthesis and optimization of a Hexa machine to reach the optimal parameters in terms of the architecture geometry that will lead to a minimal torque requirement for the actuators and a maximum overall rigidity over a required portion of the reachable workspace, like a cube with certain given dimensions. The data obtained from these further studies will give enough information to start the mechanical project of a Hexa prototype to a given application in pick-and-place operations.

7. Bibliography

- Conti, J. P.; Clinton, C. M.; Zhang, G., Wavering, A. J., 1991, "Workspace Variation of a Hexapod Machine Tool".
 Funabashi, H., 1994, "Parallel actuated mechanisms as a new robotic mechanism, Advanced Robotics, December".
 Gough, V. E., 1957, "Contribution to discussion of papers on research in automobile stability, control and tire performance", 1956-1957, Proc. Auto Div. Inst. Mech. Eng.
 Gough, 1962. Gough, V. E., Whitehall, S.G., 1962, "Universal tire test machine", In Proceedings 9th Int. Technical Congress F.I.S.I.T.A..
 Merlet, J. P., 2000, "Parallel Robots", Kluwer Academic Publishers.
 Pierrot, F., 1991, "Robots Pleinement Parallèles Légers: Conception Modélisation et Commande". Ph.D. Thesis, Université Montpellier II, Montpellier.
 Stewart, D., 1965, "A Platform with Six Degrees of Freedom". Proceedings of the Institution of Mechanical Engineers.
 Tsai, L. W., 1999, Robot Analysis: The Mechanics of Serial and Parallel Manipulators, Wiley-Interscience.
 Uchiama, M., 1994, "A 6 d.o.f parallel robot HEXA". Advanced Robotics, 8(6):601.

8. Responsibility notice

The authors are the only responsible for the printed material included in this paper.